Rearrangements of Desmosomal and Cytoskeletal Proteins During the Transition from Epithelial to Fibroblastoid Organization in Cultured Rat Bladder Carcinoma Cells

Brigitte Boyer,* Gordon C. Tucker,* Ana Maria Vallés,* Werner W. Franke,‡ and Jean Paul Thiery*

* Laboratoire de Physiopathologie du Développement, Centre National de la Recherche Scientifique and Ecole Normale Supérieure, 75230 Paris, Cedex 05, France; and ‡ Division of Membrane Biology and Biochemistry, Institute for Cell and Tumor Biology, German Cancer Research Center, D-6900 Heidelberg, Federal Republic of Germany

Abstract. Changes of cell morphology and the state of differentiation are known to play important roles in embryogenesis as well as in carcinogenesis. Examples of particularly profound changes are the conversions of epithelial to mesenchymal cells; i.e., the dissociation of some or all polygonal, polar epithelial cells and their transformation into elongate, fibroblastoid cells of high motility. As an in vitro model system for such changes in cell morphology, we have used cell cultures of the rat bladder carcinoma-derived cell line NBT-II which, on exposure to inducing medium containing a commercial serum substitute (Ultroser G), show an extensive change in their organization (epithelial–mesenchymal transition): the junctions between the epithelial cells are split, the epithelial cell organization is lost, and the resulting individual cells become motile and assume a spindle-like fibroblastoid appearance. Using immunofluorescence microscopy and biochemical protein characterization techniques, we show that this change is accompanied by a redistribution of desmosomal plaque proteins (desmoplakins, desmoglein, plakoglobin) and by a reorganization of the cytokeratin and the actin–fodrin filament systems. Moreover, intermediate-sized filaments of the vimentin type are formed in the fibroblastoid cells. We demonstrate that the modulation of desmosomal proteins, specifically an increase in soluble desmoplakins, is a relatively early event in cell dissociation and in epithelial–mesenchymal transition. In this process, a latent period of 5 h upon addition of inducing medium precedes the removal of these desmosomal components from the plasma membrane. The transition, which is reversible, is dependent on continued protein synthesis and phosphorylation but not on the presence of the inducing medium beyond the initial 2-h period. We discuss the value of this experimental system as a physiologically relevant approach for studying the regulation of the assembly and disassembly of desmosomes and other intercellular adhesion structures, and as a model of the conversion of cells from one state of differentiation into another.

ACQUISITION of cell motility is a prerequisite to biological processes taking place in tissue remodeling. It has been described as a major event in morphogenesis (22, 67, 68, 71), wound repair (75), and pathological situations such as invasion and metastasis of tumor cells (discussed in reference 62). Even though the cellular mechanisms responsible for the acquisition of cell motility remain unclear, it can be postulated that they are multiple, depending in part on the state of differentiation of the cells that will eventually migrate. Epithelial cells have two main possibilities to move: they can remain linked together and move as epithelial sheets, as observed in gastrulation and epiboly (71) and wound healing (65); alternatively, they can dissociate and migrate as individual cells. For example, during early embryogenesis certain groups of cells can detach from the epithelium and transiently or permanently express locomotory properties (8, 12, 15, 21, 64). In such cases, the acquisition of motility is correlated with dramatic changes in the program of cell differentiation. The migrating cells no longer express epithelial characteristics, and acquire a mesenchymal phenotype. This change in cell differentiation is evidenced not only by the loss of the apico-basolateral polarity typical for epithelial cells, but also by an abrupt change in cytoskeletal organization: mesenchymal cells no longer produce cytokeratin filaments and express vimentin intermediate filaments (22). In addition, the cell–cell adhesion of epithelial cells mediated by specific cell adhesion molecules (CAMs)[1] and certain junctions such as desmosomes and zonula adhaerens are decreased in transition to mesenchymal

1. *Abbreviations used in this paper*: CAMs, cell adhesion molecules; D⁻, desmosome negative; DG, desmoglein; 6-DMAP, 6-dimethylaminopurine; DP, desmoplakin; EMT, epithelial–mesenchymal transition; IF, intermediate filament; PG, plakoglobin.

cells and are strengthened in the reverse process (8, 12, 21, 22). These observations have led to the concept of "epithelial–mesenchymal transition" (EMT), defined as the possibly reversible process of conversion between epithelial and mesenchymal cell differentiation programs.

The structural and molecular mechanisms involved in such drastic changes are only poorly understood. Because of the general importance of EMT, several groups have tried to establish in vitro model systems, using well-defined cell cultures, that could be of value for studies of the individual steps of such complex processes. Although not directly relevant to EMT, many observations of enhanced migratory activity and of morphological changes of a given cell type from an epithelial to a fibroblastoid appearance have been related to effects of certain agents such as addition of antibodies against CAMs (3); transfection of cells with oncogenes (26, 55); addition of EGF, transforming growth factor-α, or "epithelial scatter factor" to cell cultures (2, 7, 61); lowering of the extracellular Ca^{++} concentration (32); or plating the cells on specific substrata (66). As a particularly convenient cell system we have used the rat bladder carcinoma cell line NBT-II which was first found to undergo EMT-like changes when cultured on collagen type I fibers (66). We have been able to demonstrate a similar effect by addition of Ultroser G, a serum substitute. As a first approach we have followed the fate of a special type of junction, the desmosome, and of junction-associated cytoskeletal elements, during an experimentally induced EMT-like change.

Desmosomes are abundant in all layers of the transitional epithelium of the bladder (i.e., the urothelium [25, 34]), and probably play an important role in maintaining tissue cohesion during mechanical stretching of this organ. In addition, the development, growth, and metastasis of bladder carcinomas has been studied extensively with respect to changes of desmosomal frequency or distribution, and of expression of cytoskeletal proteins (43, 74). The structure and composition of desmosomes has been investigated in numerous studies (for review see references 9, 20, 57), and biochemical analyses have allowed the identification of at least six major polypeptides in desmosomes of stratified epithelia including urothelium. These are the four nonglycosylated proteins: desmoplakin I (DP I, M_r 250,000), desmoplakin II (DP II, M_r 215,000), plakoglobin (PG, M_r 83,000), and a basic polypeptide of M_r 75,000 (band 6 protein). In addition three glycoproteins have been identified: desmoglein (DG, M_r 165,000), and desmocollins I (M_r 130,000) and II (M_r 115,000). Obviously these three glycoproteins are good candidates for an involvement in the formation and maintenance of stable intercellular adhesion.

Until now the only method used to study the assembly and disassembly of the individual desmosomal proteins as well as the changes in desmosomes occurring in situations of reduced intercellular adhesion was to lower the external Ca^{++} concentrations in cell culture media, resulting in the rapid internalization of desmosomes, whereas desmosomes were reformed when the Ca^{++} concentration was brought back to normal levels (13, 35, 41, 42, 50, 51, 73). As we show in this study, the EMT-like change of NBT-II cells offers a quasi-physiological model of desmosome splitting, modulation, and loss which is accompanied by enhanced cell motility and by extensive modifications of cytoskeletal organization.

Materials and Methods

Reagents

Cycloheximide, 6-dimethylaminopurine (6-DMAP), cytochalasin B, and FITC-conjugated phalloidin were purchased from Sigma Chemical Co. (St. Louis, MO). Mouse monoclonal antibodies against DPs I and II, DG, and PG have been described before (9, 10, 57). Guinea pig antiserum gpl0 is directed against cytokeratins 8 and 18. Human autoimmune antivimentin IgM was kindly provided by Prof. J. C. Brouet (Hôpital Saint-Louis, Paris, France). Rabbit antiserum against fodrin was a generous gift of Dr. J. Nelson (Institute for Cancer Research, Philadelphia, PA). Goat antiserum against rabbit aminopeptidase N, kindly provided by Dr. S. Maroux (Centre de Biochimie et de Biologie Moléculaire, Marseille, France) has been described elsewhere (17). Mouse monoclonal anticytokeratin lu5 was purchased from Boehringer Mannheim GmbH (Mannheim, FRG). Rabbit IgG against human IgM was obtained from Nordic Immunology (Tilburg, The Netherlands). FITC-conjugated goat anti-rabbit IgG (Pasteur Institute, Paris, France), FITC-conjugated rabbit anti-goat IgG (Miles Scientific, Paris, France), and Texas Red-coupled goat anti-mouse IgG (Immunotech, Marseille, France) were used as secondary antibodies. ^{125}I-labeled anti-mouse Ig, ^{125}I-labeled protein A, mouse antivimentin- and antiactin-diluted ascites were obtained from Amersham International (Buckinghamshire, UK).

Cell Culture

The NBT-II cell line originally established by Toyoshima et al. (70) was obtained from Prof. M. Mareel (Laboratory of Experimental Cancerology, University Hospital, Ghent, Belgium). The cells were grown (37°C in 5% CO_2) in standard medium (DME supplemented with glutamine, antibiotics, and 10% heat-inactivated fetal calf serum). The cells were routinely subcultured twice a week by gentle trypsinization with a solution containing 0.05% (wt/vol) trypsin 0.02% (wt/vol) EDTA, and replated at 1:20 dilution. When appropriate (see Results), Ultroser G serum's substitute (Institut Biologique Francais [IBF], Villenueve-la-Garenne, France) was added to the standard medium at a final concentration of 2%, thus defining the inducing medium. In these conditions, the growth rate curves of NBT-II cells in either standard or inducing medium were similar. In each experiment, induction of EMT was initiated after a 24-h preculture in standard medium that allowed a total recovery from trypsinization.

Cell Colonization Experiments (In Vitro Wound Model)

Subconfluent NBT-II cell monolayers were obtained after 48 h of culture in standard medium. They were gently scratched with a Gilson pipette yellow tip, and extensively rinsed with standard medium to remove all cellular debris. That procedure left a cell-free area of substratum ("wound"). Then the cultures were allowed to grow overnight in either standard or EMT-inducing medium. The next morning, the cultures were rinsed with PBS, stained with Coomassie blue, and photographed on Panatomic-X film (Eastman Kodak Co., Rochester, NY) with an Olympus camera mounted on an inverted microscope (Leitz, Wetzlar, FRG).

Immunofluorescence Microscopy of NBT-II Cells

Subconfluent monolayers of NBT-II cells were cultured on glass coverslips in either standard or inducing medium. The cells were fixed at −20°C with methanol for 5 min followed by acetone for 1 min before processing for DP, DG, PG, vimentin, cytokeratin, actin, and vinculin immunostaining. Aminopeptidase N immunolabeling was performed after fixation for 30 min in 2.5% glutaraldehyde. Before fodrin immunostaining, cells were fixed for 30 min in 1.75% formaldehyde in PBS and extracted for 5 min in 0.5% (wt/vol) Triton X-100. Primary antibodies were applied for 1 h, followed by three 5-min washes in PBS, a 30-min incubation with FITC-coupled goat anti-rabbit IgG, FITC-coupled rabbit anti-goat IgG, or Texas Red-coupled goat anti-mouse IgG, and three final washes of 5 min each in PBS. For vimentin immunostaining, primary antibody incubation was followed by application of first rabbit anti-human IgM and then FITC-coupled goat anti-rabbit IgG. Double immunofluorescence labeling was performed by applying a mixture of anti-DP and antivimentin, followed by extensive washing, incubation with rabbit anti-human IgM, washes in PBS, and

finally application of a mixture of FITC-coupled goat anti-rabbit IgG and Texas red-coupled goat anti-mouse IgG. For actin staining, FITC-coupled phalliodin was applied for 30 min, followed by several washes as described above for antibody work. Finally, coverslips were dipped briefly in water, then in ethanol, and mounted in Moviol (Hoechst GmbH, Frankfurt, FRG). The cells were viewed en face with a 63× objective using a Leitz microscope equipped with epifluorescence illumination and photographed on Tri-X pan film.

When appropriate (see Results), the percentages of D^- (desmosome negative) cells were counted. In these experiments, identical number of cells were seeded on each coverslip and the extent of confluence at the end of culture was similar as estimated by the number of cells per millimeter squared. Cells were considered D^- when DP or DG immunoreactive "dots" were totally absent from the cell periphery. For each measurement, at least 500 cells were counted.

Solubility Properties of DP, DG, and PG Proteins

Subconfluent cultures of NBT-II cells grown in standard or inducing medium in 90-mm Petri dishes were extracted sequentially. At the end of the period of cell culture, cells were transferred to 4°C, rinsed twice with ice cold PBS containing 1 mM $CaCl_2$, 1 mM $MgCl_2$, and then extracted in situ with 1 ml per Petri dish of a buffer containing 10 mM Tris-HCl (pH 7.4), 140 mM NaCl, 5 mM EDTA, 2 mM DTT, 1 mM PMSF, 0.05% Triton X-100 (near-physiological buffer) for 5 min at 4°C. Cells were scraped from the Petri dishes with a rubber policeman, homogenized with five strokes of a loose-fitting Dounce homogenizer (Kontes Glass Co., Vineland, NJ) and extraction was continued for another 5 min. The homogenate was centrifuged at 100,000 *g* for 2 h to yield a supernatant (physiological supernatant) and pellet. The latter was then homogenized by 10 strokes of the Dounce homogenizer in a buffer containing 10 mM Tris-HCl (pH 7.4), 1.5 M KCl, 5 mM EDTA, 2 mM DTT, 1 mM PMSF, 1% Triton X-100 (high salt buffer), extracted for 10 min on ice, and centrifuged at 20,000 *g* for 15 min to yield a supernatant (high salt supernatant) and pellet (insoluble fraction). For kinetic experiments (see Results), the same numbers of cells were seeded in each Petri dish. Equal numbers of cells were obtained for each time-point as estimated by counting the cells obtained in control dishes. Similar protein contents were recovered for each time-point as estimated by quantitating proteins in control dishes with the Bolton-Hunter reagent (Bio-Rad protein assay dye reagent; Bio-Rad Laboratories, Richmond, CA).

Immunoblotting

Immunoblotting with anti-DP, anti-DG, and anti-PG were performed on subcellular fractions obtained as described above. SDS-7.5% polyacrylamide gels were loaded with samples resulting from the fractionation of the same number of cells (5×10^6 cells). Immunoblotting with mouse antivimentin and guinea pig gpl0 anticytokeratin 8 and 18 was performed on total cell lysates, obtained by solubilizing the same number of cells in SDS sample buffer. Proteins were transferred electrophoretically from gels to nitrocellulose filters as described previously (69). Filters were incubated with a 1:1,000 dilution of anti-DP and anti-PG ascites, a 1:500 dilution of anti-DG ascites or gpl0 anticytokeratin antiserum for 2 h on a rotary shaker at room temperature, and rinsed extensively. The $\sim 10^6$ cpm of ^{125}I-anti-mouse IgG or ^{125}I-protein A (10 μCi/μg) were applied for 2 h at room temperature. The filters were rinsed extensively, air dried, and exposed at −80°C to XAR-5 x-ray films (Eastman Kodak Co.). The resulting autoradiograms were analyzed with a Gelscan system equipped with a scanning densitometer (LKB Instruments Inc., Bromma, Sweden). The amount of protein in each sample was within the linear range of detection.

Results

Ultroser G Induces Modification of NBT-II Cell Morphology and Motility

The NBT-II cell line is derived from a rat bladder squamous carcinoma which was first described as undergoing EMT when cultured on collagen type I fibers (66). We have found that a serum substitute (Ultroser G; IBF), added to a final concentration of 2% in the standard medium (thus defining the so-called "inducing medium"), induced the same morphological changes as collagen type I. NBT-II cells grown on glass or plastic in standard medium assumed an epithelial morphology, forming dense monolayer colonies of tightly packed polygonal cells (Fig. 1 *a*). In inducing medium, they became progressively fibroblastoid: they flattened, exhibited a spindle shape, and crawled over one another (Fig. 1, *a* and *b*).

The motility of NBT-II cells was therefore assayed by two different techniques, a colonization assay (wound healing) and time-lapse videomicroscopy. In the colonization assay, NBT-II cells cultured in standard medium were not able to cover a defined area or wound, that had been produced 24 h before, whereas NBT-II cells cultured for the same period in inducing medium invaded the wound completely (Fig. 1, *c* and *d*). The differences between the epithelial and fibroblastoid NBT-II cells in their ability to recolonize such wound areas did not arise from differences in their capacity to proliferate, since [^{3}H]thymidine incorporation into NBT-II cells cultured in either standard or inducing medium was similar: NBT-II cells cultured for 48 h in standard medium incorporated 39,933 (± 5,601 SEM) cpm of [^{3}H]thymidine added for the last 2 h of culture; whereas NBT-II cells plated and cultured in standard medium for 24 h and then in inducing medium for the last 24 h of culture incorporated, in the same experimental conditions, 36,483 (± 965 SEM cpm) of [^{3}H]thymidine. Time-lapse videomicroscopy experiments showed that cells migrated individually and did not move as groups or colony sheets. The speed of locomotion was measured more precisely: NBT-II cells cultured in standard medium did not move at all, whereas NBT-II cells cultured in inducing medium for at least 12 h reached an average speed of locomotion of 50 μm/h.

One of the major features of the EMT of NBT-II cells is the disruption of the extended cell contacts of the epithelial cells (Fig. 1, compare *a* and *b*). Since transmission electron microscopy performed on epithelial NBT-II cells in standard medium revealed the presence of numerous desmosomes in cellular interdigitations (data not shown), we studied the fate of some desmosomal proteins during EMT in special detail.

Desmosomes Are Rapidly Altered During EMT

Immunofluorescence studies performed with monoclonal antibodies against desmosome-specific proteins such as DPs I and II or DG showed that NBT-II cells cultured in standard medium expressed DP and DG immunoreactivities in typical punctate arrays along cell boundaries (Fig. 2, *a* and *d*, respectively). In addition, we examined the expression of junctional plaque proteins not confined to desmosomes: PG is shared in common by desmosomes and intermediate junctions (11); and vinculin is expressed in both intermediate junctions and focal contacts (28). Consequently, in contrast to the punctate staining of anti-DP and anti-DG, PG and vinculin immunoreactivities were distributed uniformly along cell boundaries (Fig. 2, *g* and *j*, respectively). This indicates that adhering junctions of the intermediate type, probably puncta adhaerentia, contribute, in addition to desmosomes, to the intercellular coherence of NBT-II cells.

When the standard medium was replaced by the inducing medium, the immunoreactivities found with anti-DP, anti-DG, anti-PG, and antivinculin antibodies rapidly disappeared from regions of intercellular contacts. 8 h after medium

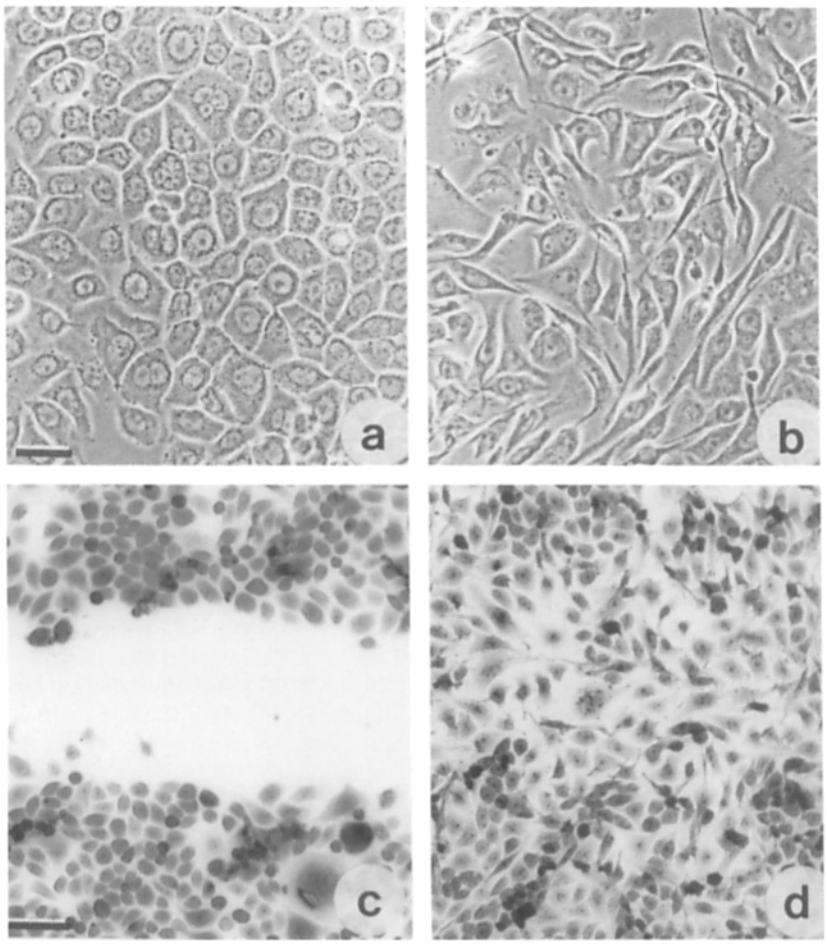

Figure 1. Effects of the inducing medium on morphology and motility of NBT-II cells. NBT-II cells cultured in either standard (*a*) or inducing (*b*) medium display distinct morphological features. Areas free of cells (wounds) made in subconfluent cell cultures were examined after 24 h of culture in either standard (*c*) or inducing (*d*) medium. Note that in *c*, the wound is not repaired; whereas in *d*, it has been totally repopulated by cells. Bars: (*a* and *b*) 10 μm; (*c* and *d*) 100 μm.

change, the majority of cells were negative, with the exception of vinculin immunostaining which persisted at certain cell contacts. Morphological changes were not yet observed (Fig. 2, *b*, *e*, *h*, and *k*). 48 h after onset of EMT, little immunostaining was seen in occasional residual contacts and the morphology of the cells was obviously transformed (Fig. 2, *c*, *f*, *i*, and *l*). It is noteworthy that in cells which had largely lost their cortical staining, DP antibodies displayed a cytoplasmic immunostaining formed by the superposition of discrete spots on a diffuse staining pattern (Fig. 2 *b*). In the same conditions, anti-DG showed only a punctate cellular staining (Fig. 2 *e*) and staining with anti-PG and antivinculin antibodies was largely diffuse throughout the cytoplasm (Fig. 2, *h* and *k*).

We estimated the percent values of cells which had lost their cortical DP staining as a function of time after initiation of EMT (D^- cells; cf. Fig. 3). Similar results were obtained from immunostainings with DG antibodies (data not shown). The relatively high basal level (23% D^- cells in cultures grown in standard medium) was mainly due to the specific conditions of culture: since DP immunostaining was more easily observable at subconfluence, experiences were performed at ~70% confluence (in these culture conditions, some isolated cells were present and did not express desmosomes). Therefore, the percent of D^- cells was compared only in cells having reached the same degree of confluence (see Materials and Methods).

During the first 4 h after medium change, there was no obvious change in the distribution of DP positive sites; i.e., desmosomes. Disappearance of cortical DP staining was first observed after 5 h of culture in inducing medium but was rather heterogeneous. Some cells were negative whereas others still showed desmosomal staining. The submembrane DP immunoreactivity was then lost very rapidly: after 8 h of culture in inducing medium, 80% of the cells were negative for cortical dot staining with anti-DP; i.e., for intact desmosomes. As shown in Fig. 2, the disappearance of cortical immunoreactivity of desmosomal marker proteins was correlated with an increase in intracytoplasmic DP-positive "dots," suggesting that the modifications of desmosome immunoreactivity were due to the rapid internalization of "half-desmosomes" occurring after initiation of EMT. To examine this hypothesis, we studied the localization of desmosomal proteins in subcellular fractions.

Modifications of Levels of Soluble and Insoluble Desmosomal Proteins

Desmosomes are known to be insoluble structures resistant to solubilization by nonionic detergents and buffers of high and low ionic strength (27). Partitioning the cytoplasm into different fractions extracted by near-physiological, Triton X-100 high salt, and SDS-PAGE buffers allowed us to demonstrate that these proteins existed in soluble and insoluble

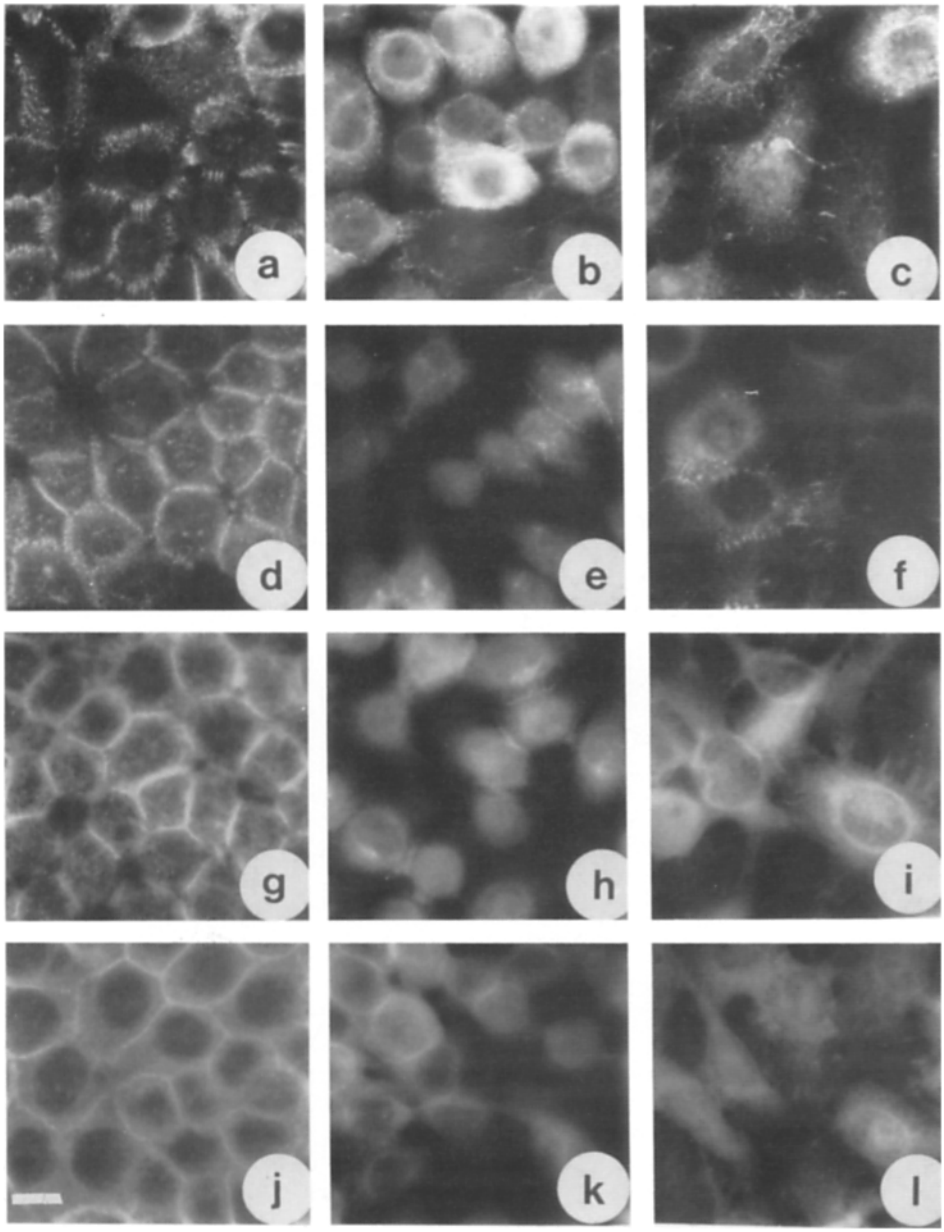

Figure 2. Disappearance of DP, DG, PG, and vinculin from the cellular cortex of NBT-II cells during EMT. Subconfluent monolayers of NBT-II cells were established in standard medium (*a*, *d*, *g*, and *j*). Alternatively they were cultured in inducing medium for various periods of time: 8 h (*b*, *e*, *h*, and *k*) or 48 h (*c*, *f*, *i*, and *l*). The cells were subsequently fixed in methanol/acetone at −20°C and processed for immunofluorescence with monoclonal antibodies directed against DP I and II (*a–c*), DG (*d–f*), PG (*g–i*), and vinculin (*j–l*) as primary antibodies followed by Texas red-coupled anti-mouse IgG as secondary antibody. Note the progressive disappearance of immunoreactivity from cellular junctions and cell periphery, and the concomitant increase of immunoreactive dots of DP and DG deep in the cytoplasm. Because of the heterogeneity of the culture, the number of cells having lost their peripheral staining does not necessarily reflect the quantificative data shown in Fig. 3. Bar, 10 μm.

forms (see also references 11, 13, 27, 50). Extraction in near-physiological and high salt buffers released certain desmosomal proteins in a soluble state (Fig. 4, *PS* and *HSS*), whereas the insoluble proteins were extracted only by the final SDS-PAGE buffer (Fig. 4, *HSI*). These insoluble proteins probably represented those proteins which were stably assembled into a cytoskeletal array and which formed the complex structures seen at the electron microscopic level. The soluble protein pool could represent either newly synthesized molecules not yet assembled into plaque structures, or the proteins disassembled from desmosomes, or a mixture of both.

Interestingly, the solubility properties of DP, DG, and PG were not identical. Under standard conditions, the soluble pool of DP molecules (~20% of the total) was released by the near-physiological buffer (Fig. 4 *A*, *PS*, lane *S*) and further extraction with high-salt buffer did not solubilize considerable additional amounts of DP (not shown). On the other hand, the near-physiological buffer did not solubilize DG molecules, as expected for an integral membrane glycoprotein (not shown). A certain proportion of DG (<10% of the total) was solubilized with the Triton X-100, high salt buffer (Fig. 4 *B*). Although present in intermediate junctions as well as in desmosomes, PG molecules were also subjected to the same analysis. As already described for other cell cultures (24), the PG soluble pool (~30% of the total) could be divided into molecules extracted by the initial near-physiological buffer and into molecules solubilized subsequently by the detergent–high salt buffer (Fig. 4 *C*, see the first lane of *PS* and *HSS*).

Immunoblotting of the subcellular fractions performed as described in Fig. 4 was done in conditions which ensured the linearity of the signal within the range of measures. The partitioning of DP, DG, and PG proteins into soluble and insolu-

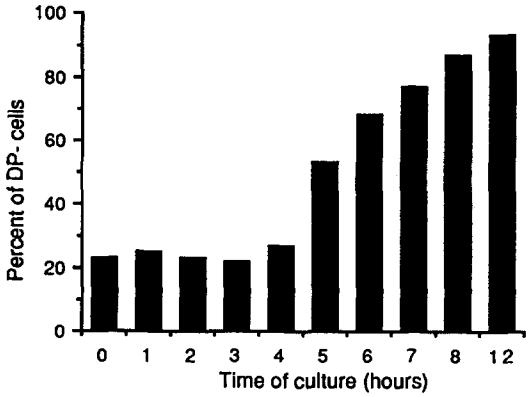

Figure 3. The rapid decay of cortical DP immunoreactivity in inducing medium is preceded by a latent period. Subconfluent cultures of NBT-II cells were established in either standard or inducing medium. Cells were fixed and processed for immunofluorescence with a monoclonal DP antibody. Cells were considered as negative (DP^- cells) when no cortical staining was visualized. The 20% background level is due to the fact that immunofluorescence studies were performed after growing cells at subconfluence.

ble forms was carried out at different time points during EMT. By scanning the autoradiograms, it was thus possible to estimate the percent of each component present in the soluble and insoluble pools during EMT. As shown in Fig. 5 *a*, the level of soluble DP changed only slightly in the first hours after EMT initiation but then increased drastically in the following 11 h, so that 16 h after medium change the cells contained twice more soluble DP than in standard conditions.

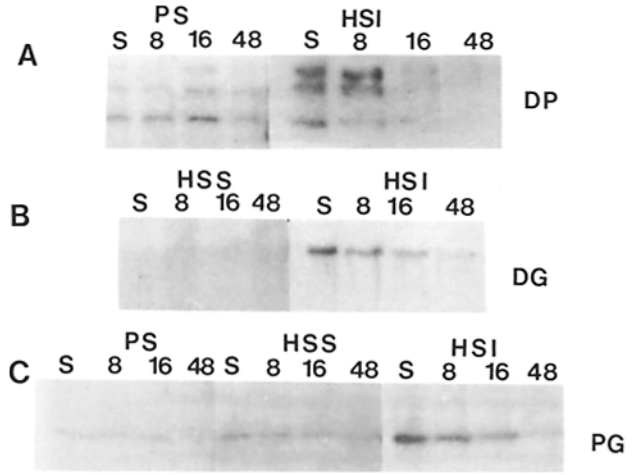

Figure 4. Levels of soluble and insoluble forms of DP, DG, and PG during EMT. Subconfluent cultures of NBT-II cells were established in standard medium (lanes *S*). Alternatively, they were cultured in inducing medium for 8, 16, or 48 h. Cells were then lysed and fractionated in situ with near-physiological and Triton X-100, high-salt buffers to yield a physiological supernatant (*PS*), high salt supernatant (*HSS*), and insoluble fraction (*HSI*). The proteins solubilized in SDS-containing buffer were separated by SDS-PAGE and immunoblotted with DP (*A*), DG (*B*), and PG (*C*) antibodies. Since extraction with high salt buffer does not release substantial amounts of DP protein in soluble form, and extraction with near-physiological buffer does not solubilize DG protein, the corresponding autoradiograms have not been shown.

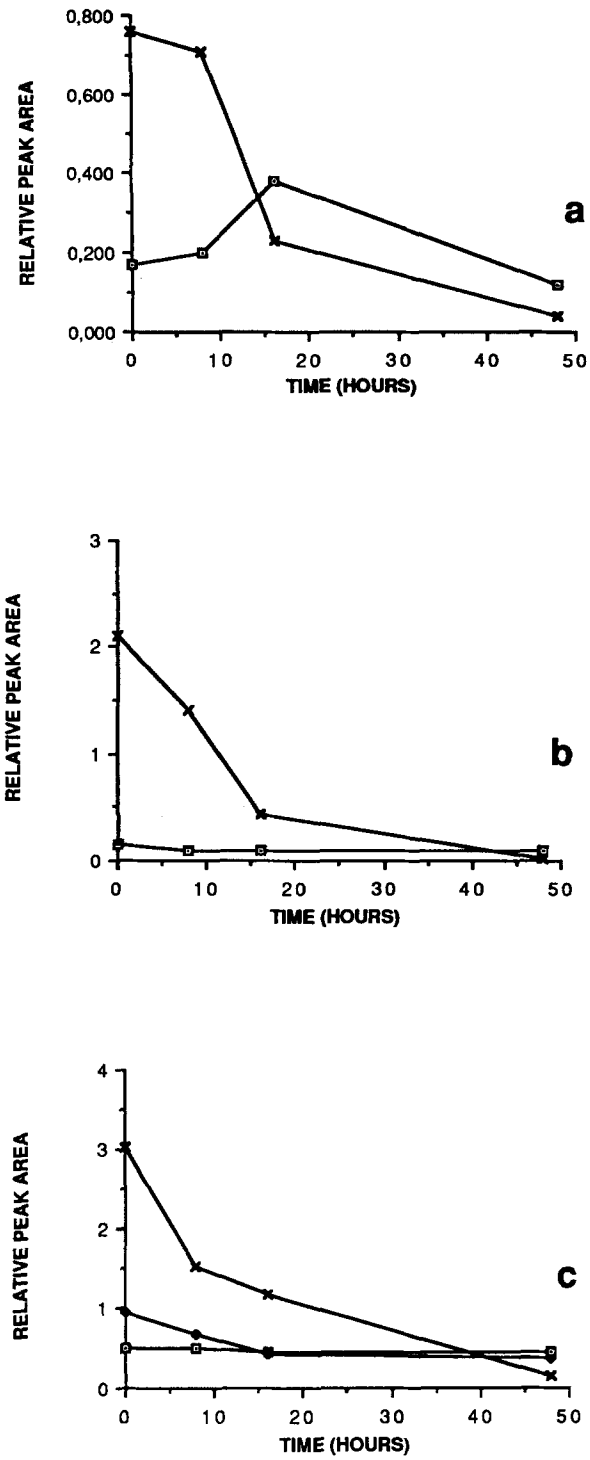

Figure 5. Modifications of levels of DP, DG, and PG in soluble and insoluble forms during EMT. Subconfluent monolayers of NBT-II cells were fractionated into a physiological supernatant (⊡), high salt supernatant (♦), and insoluble fraction (×). Each lysate for each time-point was divided into equal aliquots which were separated by SDS-PAGE and immunoblotted with anti-DP (*a*), anti-DG (*b*), and anti-PG (*c*). The immunolabeled DP, DG, and PG were quantitated as described in Materials and Methods. Values are expressed as the calculated peak areas resulting from scanning the autoradiograms.

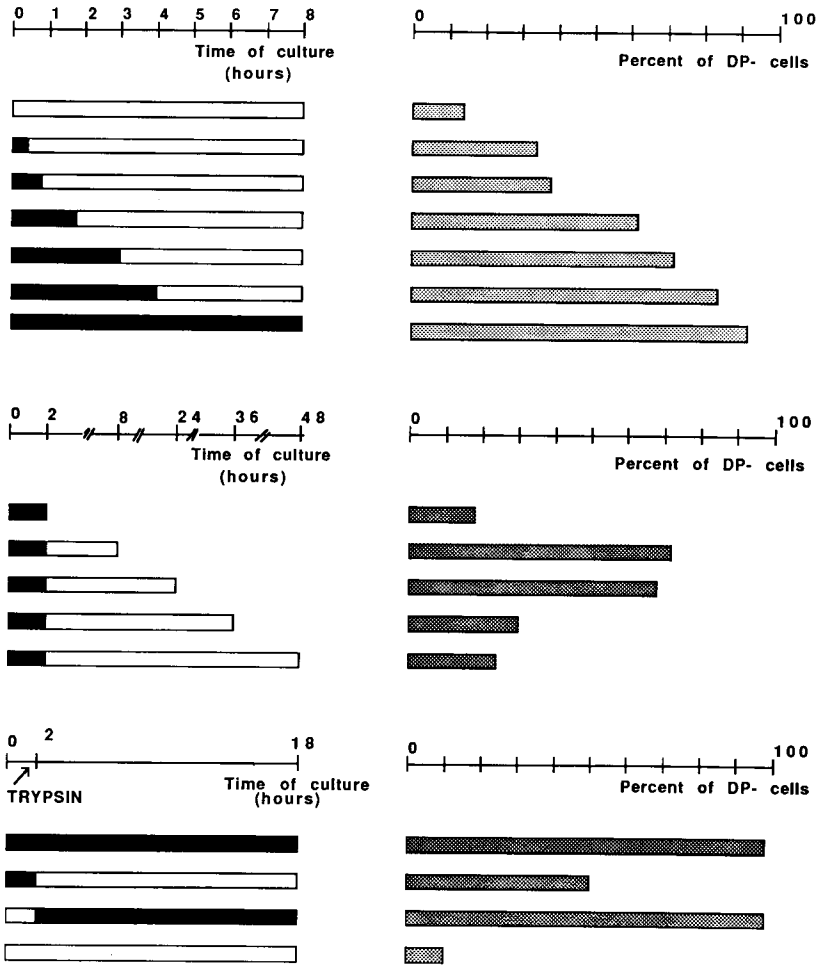

Figure 6. A short pulse of treatment with inducing medium is sufficient to induce the change in DP distribution. Subconfluent monolayers of NBT-II cells were cultured in either standard or inducing medium for various periods of time. The black boxes on the left represent the duration of the pulse of inducing medium and the white boxes on the left the duration of the subsequent culture in standard medium. In *a*, the cells were pulsed with the inducing medium for various periods of time and examined for DP immunofluorescence after 8 h of culture. In *b*, the cells were pulsed for 2 h with the inducing medium and were incubated subsequently in standard medium for periods up to 46 h. In *c*, the cells were pulsed for 2 h with the inducing or standard medium. They were then trypsinized with 0.05% trypsin and 0.02% EDTA, plated on glass coverslips, and incubated for another 16 h in standard or inducing medium. Each line on the right side represents the percent of cells without cortical DP immunostaining (*DP⁻ cells*), which were grown in the conditions defined in the corresponding line to the left.

The membrane-bound glycoprotein DG showed a different kind of change of its solubilization properties (Fig. 5 *b*). Until 16 h after EMT initiation, a significant proportion of it remained in a pelletable form that could not be extracted in the Triton X-100 high salt buffer used. Thereafter, however, the relative proportion of insoluble fraction as well as the absolute amount of DG decreased drastically. This indicated that the state of DG is altered upon the internalization of the desmosomal material.

An even different solubilization behavior was found for PG. The PG pool soluble in near-physiological buffer remained essentially unaltered (Fig. 5 *c*) whereas the high salt-extractable and insoluble pools decreased significantly. As a result, 48 h after the onset of EMT the form soluble in the near-physiological buffer exceeded the insoluble PG.

Internalization of Desmosomal Proteins Requires only a Short Pulse of Inducing Medium and Can Be Reversed in Standard Conditions of Culture

NBT-II cell dissociation by inducing medium exhibited some features which were different from those observed after lowering the Ca^{++} concentration in the culture medium: in low calcium medium, DP and DG immunoreactive sites were totally internalized in <1 h, whereas a considerable proportion of the PG and vinculin immunoreactive structures remained at the cell surface (data not shown). We therefore decided to define some prerequisites of the system in order to understand how the signal provided by the inducing medium acts in the cell and on the desmosomes.

In a first set of experiments, we applied a pulse of inducing medium for various periods (up to 8 h) followed by culture in standard medium. We estimated the effect on desmosomes by counting the number of cells without cortical DP immunoreactivity after a total of 8 h in the culture conditions defined above. As shown in Fig. 6 *a*, a 30-min or 1-h pulse did not induce obvious desmosome losses. 2- and 3-h pulses, however, led to desmosome disappearance in 40 and 50% of the cells, respectively. In comparison, the continuous presence of the inducing medium for 8 h led to DP internalization and desmosome loss in 70% of the cells.

In a second set of experiments, NBT-II cells were pulsed for 2 h with the inducing medium and then incubated for varying periods in standard medium. The number of cells without DP reactive sites at the cell periphery (Fig. 6 *b*) decreased with time of culture in the standard medium and reached the basal level (identical to that obtained without inducing medium) after 46 h of chase with the standard medium. We conclude, therefore, that the loss of desmosomes, which cannot be observed before several hours of culture, occurs even if the inducing medium is not applied during the whole incubation period but is totally reversible by culturing the cells back in standard medium during an appropriate period of time; i.e., for 2 d.

To rule out the possibility that the long-term inducing

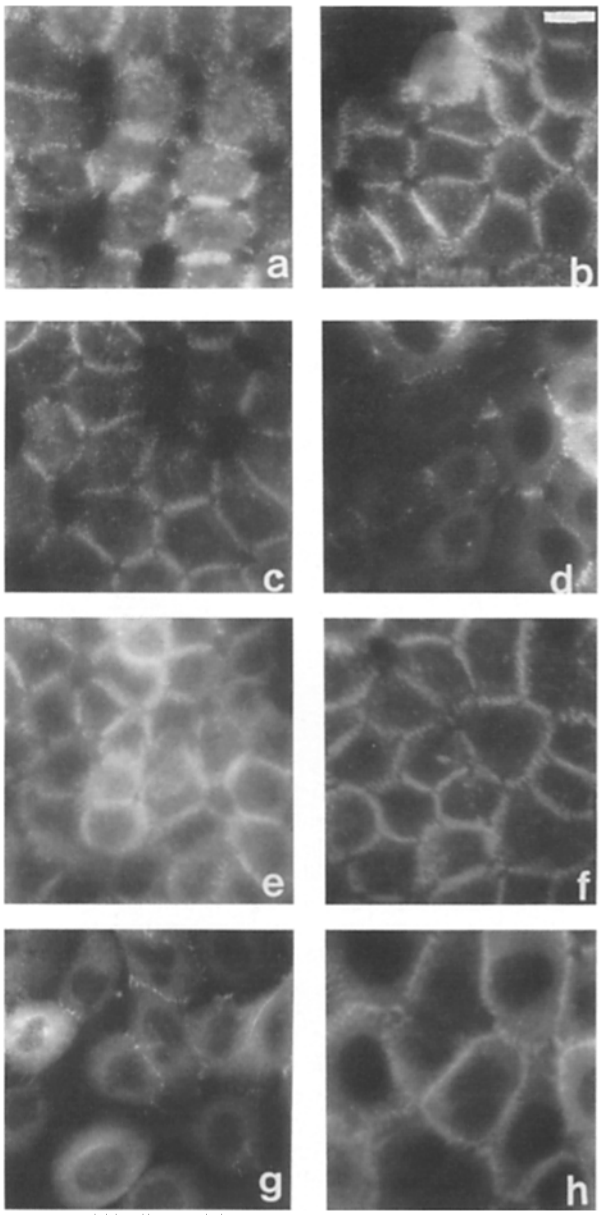

Figure 7. The change in DP distribution is dependent on phosphorylation and protein synthesis. Subconfluent monolayers of NBT-II cells were established for 6 h in standard medium (*e*), in standard medium containing 1 mM cycloheximide (*a*) or in standard medium containing 600 μM 6-DMAP (*f*). Alternatively, the cells were cultured for 6 h in inducing medium in the absence of inhibitors (*g*), in the presence of 1 mM cycloheximide added throughout the period of culture (*b*), in the presence of 1 mM cycloheximide added for the first 3 h (*c*), in the presence of 1 mM cycloheximide added for the last 3 h (*d*), or in the presence of 600 μM 6-DMAP (*h*). The cells were fixed and processed for immunofluorescence using a monoclonal DP antibody. Note that neither cycloheximide nor 6-DMAP alters the peripheral distribution of DP in cells grown in standard medium. In contrast, they inhibit desmosome internalization and loss triggered by the inducing medium. Bar, 10 μm.

effect was due to the slow release of inducing factors from the extracellular matrix synthesized by NBT-II cells, we carried out a third set of experiments (Fig. 6 *c*). After a 2-h incubation in either standard or inducing medium, cells were trypsinized, washed extensively, plated on coverslips, and cultured for another 16 h in standard or inducing medium. As illustrated in Fig. 6 *c*, control cells pulsed and cultured in standard medium after trypsinization were able to reform desmosomes at the end of the incubation. On the other hand, desmosomes were internalized or lost in 50% of the cells first pulsed with inducing medium, and then trypsinized and cultured in standard medium.

Together, these results indicate that the signals provided by the inducing medium reach the cell rapidly, suggesting that the cellular modifications in response to the inducing signals are not leading immediately to cell dissociation and loss of desmosomes.

Internalization of Desmosomes Requires Protein Synthesis and Phosphorylation

Cycloheximide, an inhibitor of protein synthesis, was added to cells grown in inducing medium for 6 h. Desmosome disappearance was estimated by the loss of DP reactive sites at the cell periphery. When 1 mM cycloheximide was present throughout the incubation period in the inducing medium, no desmosome losses were observed (Fig. 7 *b*). The same blocking effect was obtained when 1 mM cycloheximide was added for the first 3 h of incubation and then removed from the cell culture by extensive washing (Fig. 7 *c*). In contrast, when added for the last 3 h of the incubation period, cycloheximide did not have any effect on desmosome modulation (Fig. 7 *d*). We checked, by [^{35}S]methionine incorporation experiments done in parallel, that the presence of cycloheximide in the culture medium totally blocked protein synthesis, whereas removing the drug from the cell culture restored it (data not shown).

We tested also the effect of 6-DMAP, an inhibitor of diverse cellular kinases (45), on the internalization of desmosomes in the inducing medium. Used at concentrations ranging from 20 μM to 1 mM, 6-DMAP did not inhibit [^{35}S]methionine incorporation into NBT-II cells and at concentrations up to 800 μM it inhibited only slightly [^{3}H]thymidine incorporation (data not shown). When used at high concentrations (600–800 μM) 6-DMAP abolished the effect of the inducing medium on desmosomes (Fig. 7 *h*). In control cells cultured in standard medium, the addition of 6-DMAP did not modify substantially the distribution of DP immunoreactive sites (Fig. 7 *f*). The inhibitory effect observed with 6-DMAP did not result from the partial inhibition of proliferation since drugs such as hydroxyurea, which totally inhibited [^{3}H]thymidine incorporation into NBT-II cells had no effect on desmosome internalization (data not shown).

These results suggest that protein synthesis and phosphorylation events are necessary steps in the pathway leading to desmosome disruption and internalization.

Modifications of Cytoskeletal Organization During Cell Dissociation

The cytoskeleton is likely to be involved in EMT-like changes of cell organization for two main reasons. First, microfilament organization plays a major role in the acquisition of motility (38). Second, desmosomes anchor intermediate filaments (IFs) to the cell surface (e.g., reference 5). Therefore, it was interesting to study the distribution of the actin filament system and the IF cytoskeleton in epithelial and fibroblastoid NBT-II cells.

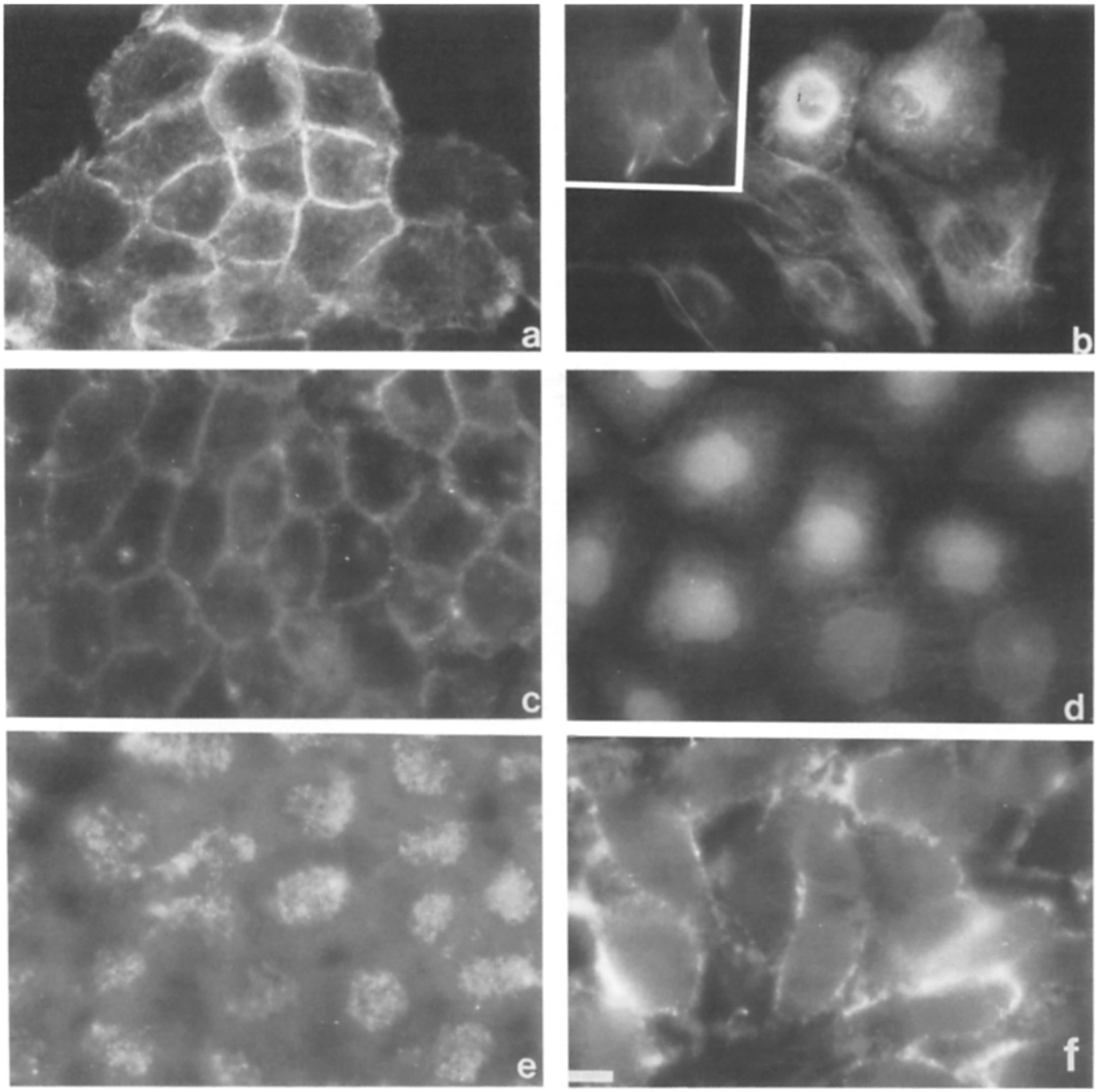

Figure 8. Changes of cytoskeletal elements in epithelial and fibroblastoid NBT-II cells. Subconfluent monolayers of NBT-II cells were maintained in either standard (*a*, *c*, and e) or inducing (*b*, *d*, and *f*) medium, fixed, and processed for immunofluorescence microscopy. (*a* and *b*) Actin was visualized using FITC-labeled phalloidin. Note actin enrichment along cell boundaries in *a* but not in *b*. The inset in *b* shows a well-spread fibroblastoid cell exhibiting actin staining with several focal contacts. (*c* and *d*) For fodrin immunostaining, cells were fixed in formaldehyde (1.75%) and permeabilized with Triton X-100. Photographs shown here were taken at the basolateral plane of the cells. Note peripheral enrichment at cell boundaries in *c* and a central, mostly perinuclear concentration in *d*. (*e* and *f*) Aminopeptidase N immunoreactivity was visualized on the apical surface of epithelial cells (*e*), whereas it was distributed uniformly on the entire cell surface of fibroblastoid cells (*f*). Bar, 5 μm.

The distribution of actin was primarily subcortical in the epithelial cell cultures (Fig. 8 *a*). It became less organized in fibroblastoid cells appearing upon growth in inducing medium. In some cells, stress fibers formed by actin bundles were visualized, whereas in other cells, the pattern was more disperse (Fig. 8 *b*). Actin bundles were localized predominantly at the edges of some well-spread fibroblastoid cells (Fig. 8 *b*, *inset*), with a pattern similar to that found in focal contacts.

We also studied the distribution of fodrin, the structural and probably functional homologue of spectrin in nonerythroid cells (29). As shown in Fig. 8 *c*, fodrin immunostaining was prominent in the regions of cell contacts, and focusing at the apical and basal planes indicated that it was predominantly localized at the basolateral membrane. The polarized staining was lost as early as 8 h after addition of the inducing medium. Little or no fodrin was detected in regions of apposition of adjacent cells, and the fodrin immunostaining assumed a diffuse distribution enriched in the perinuclear region (Fig. 8 *d*).

Aminopeptidase N, which is localized at the apical surface of rabbit intestinal cells (30), assumed a partially polarized

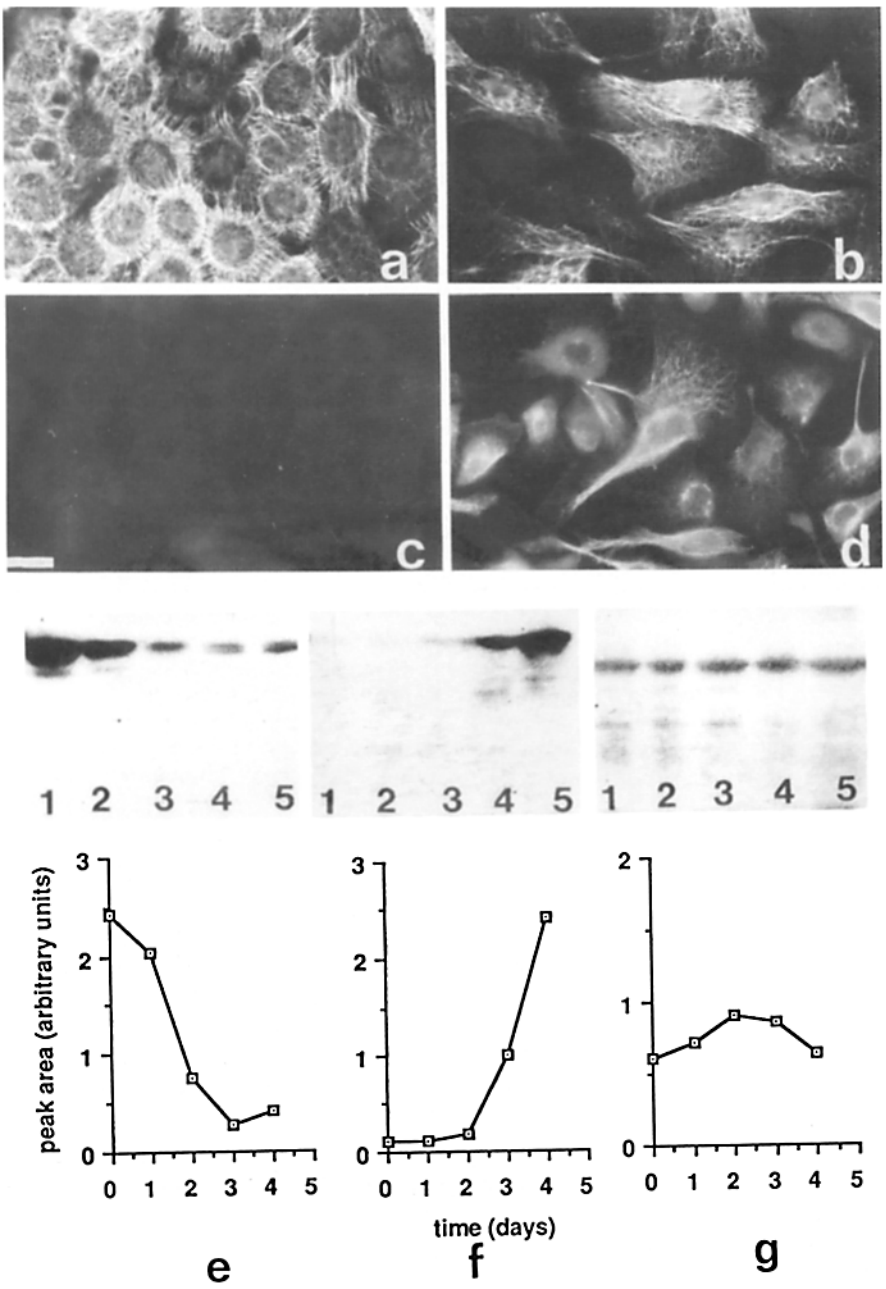

Figure 9. Expression of intermediate filaments in epithelial and fibroblastoid NBT-II cells. Subconfluent monolayers of NBT-II cells were maintained in either standard (*a* and *c*) or inducing (*b* and *d*) medium, fixed, and processed for immunofluorescence microscopy using a monoclonal cytokeratin antibody (lu-5) (*a* and *b*) or a human autoimmune antiserum against vimentin (*c* and *d*). Note typical epithelial fibril organization in *a*, with anchorage sites at desmosomes, as compared to a less ordered display in *b*. Vimentin filaments are not detected in epithelial cells (*c*) but are intensely stained in fibroblastoid cells (*d*). (*e*, *f*, and *g*) 20 μl of total lysates corresponding to a constant number of cells harvested from cultures in standard medium (lane *1*) or from cultures induced for 1 to 4 d (lanes *2* to *5*, respectively) were subjected to gel electrophoresis and immunoblotting (upper part) performed using monoclonal antibodies against cytokeratins 8 and 18 (*e*), vimentin (*f*), and actin (*g*). The resulting autoradiograms were scanned by densitometry and the peak areas calculated (lower part). Note that the steady-state level of cytokeratin proteins decreases as vimentin expression increases. As an internal control, actin expression remains roughly constant during EMT. Bar, 10 μm.

distribution on the plasma membrane of NBT-II cells: its immunoreactivity was observed predominantly at the apical surface (Fig. 8 *e*); this restricted distribution was lost upon growth in inducing medium and the immunoreactivity was redistributed on the entire cell surface (Fig. 8 *f*).

The organization of cytokeratin IFs in epithelial and fibroblastoid forms of NBT-II cells was studied with cytokeratin antibodies (Fig. 9, *a* and *b*) as well as with a guinea pig antiserum specifically directed against cytokeratins 8 and 18 (data not shown). In the epithelial cell colonies, the cytokeratin filaments displayed a very organized distribution: the antibodies stained fibrils extending from the cell surface to the perinuclear region, many of them showing an almost radial distribution (Fig. 9 *a*). The fibroblastoid cells exhibited dramatic differences of cytokeratin filament organization. The overall immunostaining with both kinds of antibodies was greatly reduced and the fibrils formed a disorganized cytoplasmic meshwork which apparently had lost its membrane anchorage (Fig. 9 *b*).

Vimentin was not detected in NBT-II epithelial cells (Fig. 9 *c*). However, after 2 d of culture in the inducing medium, vimentin IFs were observed in many cells, whereas other cells had a more diffuse pattern of staining (Fig. 9 *d*). Immunoblotting experiments performed with antibodies specific for cytokeratins 8 and 18 and vimentin confirmed the progressive reduction of cytokeratins and the appearance of vimentin during EMT. Quantification of the amounts of cytokeratins and vimentin expressed during EMT was done by scanning the autoradiograms (Fig. 9, *e* and *f*). As early as 1 d after addition of the inducing medium, the amount of cytokeratin was already reduced, whereas vimentin expression was not yet initiated. Vimentin expression was visual-

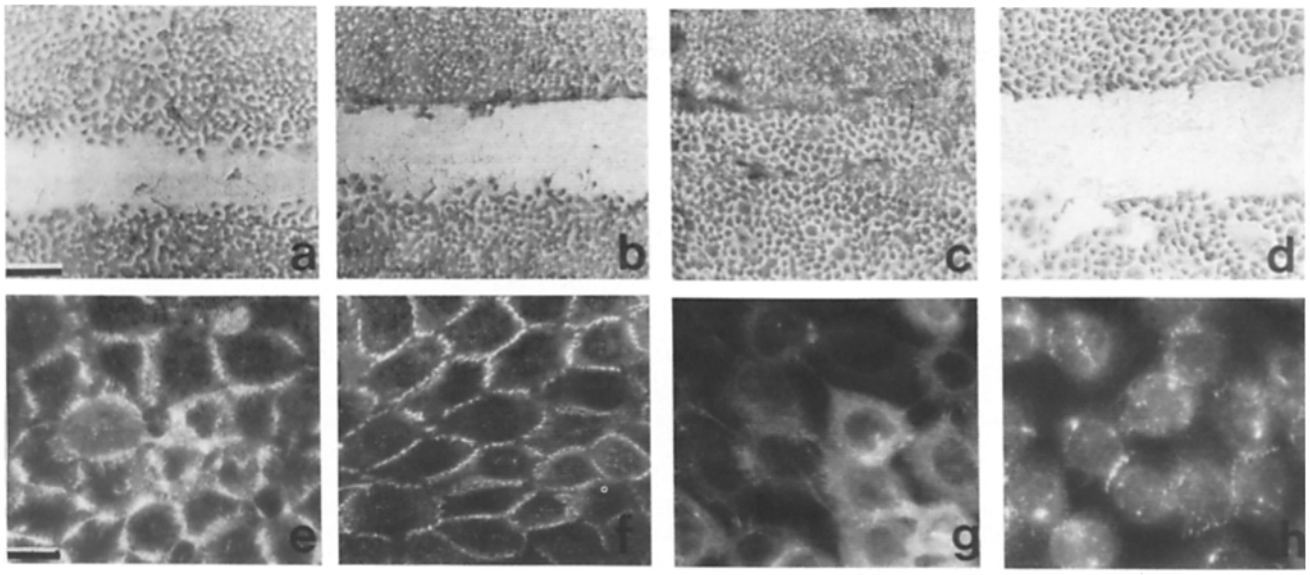

Figure 10. Disruption of cell contacts and changes in desmosomes are not dependent on cell movement. Subconfluent monolayers of NBT-II cells were established in either standard (*a*, *b*, *e*, and *f*) or inducing medium (*c*, *d*, *g*, and *h*) for 16 h. Cells were cultured in the absence (*a*, *c*, *e*, and *g*) or presence (*b*, *d*, *f*, and *h*) of cytochalasin B (1 μg/ml). (*a–d*) In one set of experiments, the cultures were scratched gently in order to create wounds and photographs of the wounds were taken at the end of the incubation. Control cells cultured in standard medium do not migrate into the cell-free area (*a* and *b*), whereas cells grown in inducing medium have totally covered it (*c*). The migration of cells grown in inducing medium is inhibited by cytochalasin B (*d*). (*e–h*) In a parallel set of experiments, cells were fixed and processed for DP immunostaining. Note that the cells grown in inducing medium are elongated in the absence of cytochalasin B (*g*), whereas in the presence of cytochalasin B (*h*) they are dissociated but do not exhibit pseudopodial protrusions. Bars: (*a–d*) 100 μm; (*e–h*) 10 μm.

ized by immunoblotting 2 d after initiation of the transition and then increased dramatically. 3–4 d after initiation of the transition, the expression of cytokeratin proteins was strikingly lowered but not totally abolished. This result confirms the immunofluorescence data, showing the persistant but much lower expression of cytokeratins in fibroblastoid NBT-II cells together with the appearance of vimentin fibrils.

Desmosome Loss Is not Necessarily Related to Acquisition of Cell Motility

Since cell dissociation, desmosome changes, acquisition of motility, and alterations in the cytoskeletal organization occurred roughly at the same time during EMT, it was important to know whether the disruption of intercellular contacts and the rearrangement of desmosomes were merely a consequence of the mechanical stresses exerted by cells in movement. To answer this question, we carried out a series of experiments in which cell motility was inhibited by cytochalasin B and the cells examined for DP immunoreactivity. We used cytochalasin B at 1 μg/ml, which was found not to inhibit [^{35}S]methionine incorporation during the 16-h experiment and which inhibited [^{3}H]thymidine incorporation by only 50% (data not shown). Up to 1 μg/ml, cytochalasin B had no detectable effect on the morphology and DP immunoreactivity of epithelial NBT-II cells cultured in the standard medium (Fig. 10, compare *a* and *e* with *b* and *f*). Motility of NBT-II cells grown in the presence of cytochalasin B was tested by the colonization assay described above. For concentrations ranging from 0.4 μg/ml to 1 μg/ml, cytochalasin B prevented NBT-II cells cultured in the inducing medium from penetrating into cell-free areas provided by cell culture wounds (Fig. 10, compare *c* and *d*). However, at the same concentrations, it was not able to inhibit desmosome disruption and internalization (Fig. 10, compare *g* and *h*). In the presence of cytochalasin B, the cells cultured in the inducing medium were obviously dissociated, although they did not elongate or spread (Fig. 10 *h*). Since the cell colonization assay assessed the motility of NBT-II cells rather than their proliferation rate, these results suggested that desmosome alterations, although coincident with the acquisition of motility were not a direct consequence of it.

The Transition Towards a Fibroblastoid Phenotype Is Reversible

The maintenance of the fibroblastoid phenotype was strictly dependent on the continuous presence of the inducing medium. Whatever the duration of culture in inducing medium, fibroblastoid cells were able to reacquire their epithelial differentiation provided that the inducing medium was replaced by standard medium. Immunofluorescence microscopy was performed with anti-DP and antivimentin on cell cultures which were maintained for 2 mo in the inducing medium and grown back in the standard medium for 3 d. In clusters of cells appearing upon growth in standard medium, no extended vimentin IF staining was detected (Fig. 11 *a*). In these cells, a punctate peripheral staining typical of that observed for desmosomes was observed with anti-DP immunolabeling (Fig. 11 *b*). This result suggests that the transition to the mesenchymal phenotype could be fully reversed by removing the inducing medium. The long period of time required for the disappearance of vimentin IFs most likely reflects the high stability of these filaments and the longevity of the protein (4).

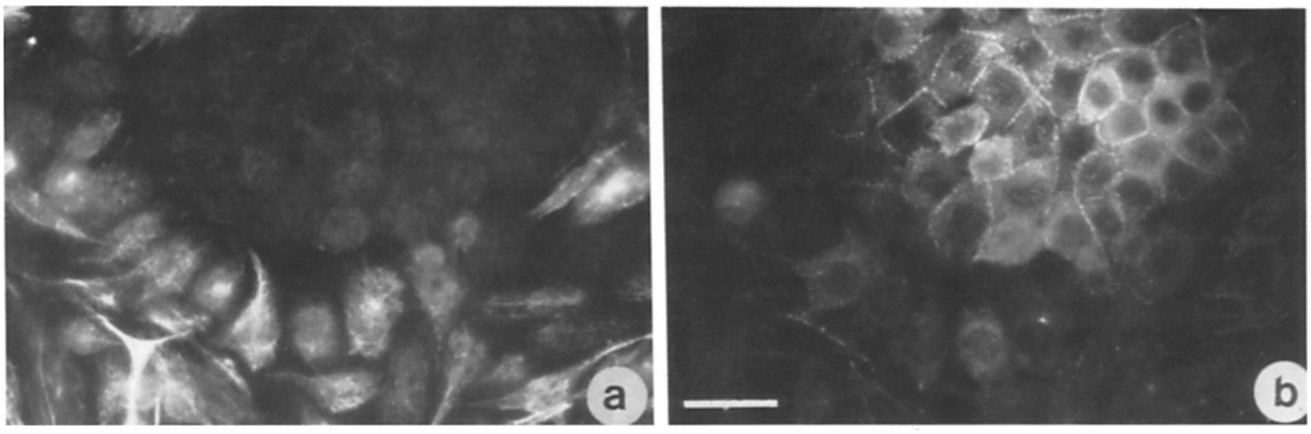

Figure 11. The transition towards a fibroblastoid phenotype is reversed by removing the inducing medium. NBT-II cells were maintained in inducing medium for 2 mo before switching to standard medium for 3 d. Cells were fixed and processed for double immunofluorescence microscopy using a human autoimmune antiserum against vimentin (*a*) and a monoclonal antibody against DPs (*b*). Note recovery to vimentin-negative state in the peripheral epithelial cell colony (*a*) which exhibits DP immunolabeling in a peripheral punctate pattern typical of localization of the immunoreactivity in desmosomal intercellular junctions (*b*). Bar, 25 μm.

Discussion

Understanding the mechanisms involved in the change of cell organization from an epithelial to a fibroblastoid appearance (EMT) whereby the orderly activation or suppression of genes in response to environmental signals leads to cell dissociation and motility remains a crucial issue in embryology. We have been able to demonstrate that soluble factors contained in Ultroser G, as well as insoluble extracellular matrix components (66; Tucker, G. C., B. Boyer, J. Gavrilovic, H. Emonard, and J. P. Thiery, manuscript in preparation), induce such a conversion in an in vitro cell culture model system; i.e., the NBT-II cell line derived from a rat bladder carcinoma (70). Our major goal is now to purify the soluble factors promoting multiple effects such as cell dissociation and motility, and to understand what is the hierarchy of the events leading to EMT. Apparently, the NBT-II cell model system fulfills several major criteria of EMT as described in other systems.

First, we show that addition of inducing medium (containing Ultroser G) induces morphological changes resembling those observed in embryonic cells undergoing EMT. Before addition of inducing medium, the cells form a cobblestone-like monolayer of polygonal cells; whereas upon addition of inducing medium, the cells dissociate, assume a spindle-like shape, and migrate actively as individual cells.

Second, the changes in cytoskeletal organization also correspond to a change from an epithelial to fibroblastoid character. In standard medium, NBT-II cells form an epithelial-like sheet, as indicated by the enrichment of fodrin, a marker of the basolateral domain of the plasma membrane (46), at the basolateral plasma membrane; as well as by the predominantly apical localization of aminopeptidase N; and by the observation that in immunofluorescence microscopy, PG and vinculin are enriched in extended, linear boundary structures at the level of the subapical cortex, resembling a zonula adhaerens.

Third, NBT-II cells contain a well-developed network of cytokeratin IFs, most of which radiate from the perinuclear cytoplasm toward the periphery, where they frequently terminate as discrete spots near the plasma membrane; i.e., desmosomes. After induction of EMT, the cytokeratin fibril distribution is dramatically altered and no longer shows preferential order. However, even though expressed in lower amounts, cytokeratins do not disappear completely from the fibroblastoid NBT-II cells. Probably, some of these residual cytokeratin IFs are anchored to the plaques associated with the intracytoplasmic, desmosome-derived vesicular structures, as described for other individualized epithelial cells separated by treatment with Ca^{++}-chelating agents, or with trypsin, or after growth in media of low calcium concentrations (13, 35, 41, 42, 49). Electron microscopy studies are underway to clarify this point.

Fourth, vimentin IFs are formed in the fibroblastoid NBT-II cells relatively early upon EMT induction. Such a rapid induction of vimentin IF formation has been often observed in primary cultured epithelial cells (59) including rat hepatocytes (24), as well as human mesothelial and urothelial cells, and this advent of vimentin is known to be influenced by various components such as externally added retinoid compounds as well as certain growth factors and hormones (for reviews see references 37, 53, 54). Since it has been demonstrated that vimentin IFs may be linked to desmosomes (10, 25, 36), the desmosome-derived structures detected in the cytoplasm of the fibroblastoid NBT-II cells could be associated with vimentin as well as with cytokeratin filaments. Induction of synthesis of vimentin in carcinoma cells is also of interest since the onset of vimentin synthesis has been correlated in some carcinoma cells with the acquisition of metastatic properties (52).

Fifth, actin is another cytoskeletal protein whose change in distribution is indicative of EMT: after addition of the inducing medium, the cortical ring of actin microfilaments disappears and is replaced by stress fibers in the long axis of cells, typical of many mesenchymal cells in culture (6).

Taken together, these changes of cytoskeletal characteristics indicate that the NBT-II model provides a meaningful system in which to analyze possible biochemical and genetic mechanisms involved in EMT. It should be noted, however, that none of the above mentioned criteria alone defines a

change to a state of a cell comparable to the complete developmental program of a mesenchymal cell in embryogenesis, nor does it exclude an epithelial cell character: individual or loosely interconnected cultures of round or elongated, spindle-shaped cells have been described for various cell cultures derived from epithelial cells, including cells from thymic reticulum (40, 56, 63), mesothelium (19, 36, 37), mammary gland epithelium (58), amniotic fluid (48), as well as carcinoma cells floating in—and cultured from—pleural fluids or ascites (52). Clearly, the continual expression of some cytokeratins, and the presence of cytokeratin IFs, per se are not inhibitory to cell motility in vitro as indicated by the presence of cytokeratin IFs in certain cultured fibroblastoid or even smooth muscle-like cells (1).

Alterations of Desmosomal Components During Cell Dissociation and EMT

The role of the extracellular matrix in the transient ability of NBT-II cells to migrate is currently under study (Tucker, G. C., B. Boyer, J. Gavrilovic, H. Emonard, and J. P. Thiery, manuscript in preparation). In the present study, we have focused our interest on possible mechanisms that contribute to NBT-II cell dissociation. Clearly, intercellular adhesion of epithelial cells is mediated by CAMs and special junctions. The modulation of CAMs during EMT has been well documented in vivo (12), and it has been suggested from in vitro transfection experiments that transfection of the liver cell adhesion molecule (L-CAM) provides a mechanism for aggregation of cells. However, it is also clear that the formation of epithelial sheets does not depend exclusively on CAM expression (16, 44). Thus, cell adhesion in epithelial sheets must involve other components, and here the constituent molecules of junctions are obvious candidates. Among the specialized junctions, desmosomes seem to play a crucial role in the establishment and maintenance of epithelial sheets, although it is not yet clearly established which desmosomal components are actually involved in cell adhesion (27). Our present results show extensive alterations of desmosomal structures and proteins during EMT, whereas the disappearance of vinculin from the cell cortex, which is probably confined to intermediate junctions, is a later event. The mechanisms by which Ultroser G acts to promote desmosomal changes is most probably a multistep cascade, as suggested by our immunofluorescence microscopic studies of cells grown in various culture conditions. We demonstrate that a 5-h period of latency follows the addition of Ultroser G and that desmosomal splitting and partial disassembly is subsequently achieved in the ensuing 3 h. The 5-h latency period obviously exceeds the time needed for the interaction of Ultroser G with the cells since a 2-h pulse of inducing medium has a notable effect on desmosomes which is then observed several hours after removing the inductor from the culture medium. During this 2-h period the inductor probably remains associated with cells, and is not trapped in the extracellular matrix, as trypsinization of NBT-II cells pulsed for 2 h with inducing medium did not prevent desmosome changes. Moreover, we have shown that the pathway leading to desmosome alterations includes phosphorylation and the action of certain limiting proteins as indicated by the effects of some specific inhibitors of phosphorylation and protein synthesis. Obviously, analysis of the proteins accumulating in NBT-II cells in response to inducing medium is needed to give further insight into the mechanisms by which the inducing medium produces desmosome alterations.

As a first step we have studied, by immunolocalization and immunoblotting of proteins of subcellular fractions, the fate of desmosomal proteins during EMT. Immunolocalization of DPs I and II reveals that cortical (i.e., desmosome-associated DP) is internalized during EMT and appears as discrete intracytoplasmic spots which most likely represent endocytic vesicles bearing remnants of desmosomal plaques (cf. references 13, 35). The vesicle nature is also indicated by the appearance of DG, a transmembrane protein, in such dots (cf. this study and reference 13). Concomitantly, there is a notable increase in the diffuse cytoplasmic immunofluorescence with DP antibodies, similar to that observed upon exposure of cells to low calcium concentrations (35, 41, 42, 50). Biochemical analyses suggest that during this period of time a considerable portion of DP is solubilized, since the soluble DP pool increases for the first hours of EMT, whereas the proportion of insoluble DP decreases. We suggest therefore that solubilization of DP might play a key role in the destabilization of desmosomes. Studies of the rates of synthesis and turnover of the various desmosomal proteins, in pulse and pulse–chase experiments, are now underway to identify more precisely the desmosomal target(s) involved in these changes.

In the last decade, the problem of assembly and disassembly of desmosomes and desmosomal plaques has been approached primarily by calcium switch experiments (32, 35, 41, 42, 50). However, the specific regulation of desmosome formation and disassembly may depend on the cell type used and on the specific inductor of the switch. The NBT-II model system thus provides an alternative physiologically relevant method to study the reversible process of desmosome assembly and disassembly. Obviously, there also exist other factors that can affect, or at least contribute to, the dispersion of cells from a tightly packed cobblestone monolayer to a population of motile individual cells, such as the "scatter factor" described by Stoker and colleagues (60, 61). Future experiments will reveal whether these different factors interact separately with distinct receptors or whether there are interrelationships forming effector networks.

Our observations made with the NBT-II rat bladder carcinoma cells grown in culture may also be relevant for our understanding of two major events in cancer spreading and malignant growth; i.e., invasion and metastasis on the one hand and the progressive appearance of tumor cell type heterogeneity on the other (for reviews see references 18, 33, 47). Local, and usually transient, loss of intercellular adhesion, including the splitting of desmosomes, is an obvious prerequisite for the invasion of carcinomas and for metastasis to distant sites, and this spreading of tumor cells is apparently facilitated by a higher motility of the invasive and metastatic cells. Moreover, changes of the morphological appearance and the state of differentiation of cells within a tumor similar to those described in the present study will give rise to intrinsic tumor cell heterogeneity, which may also include differences in the expression program and would explain the known, puzzling phenomenon of the emergence of different kinds of tumors from a certain primary carcinoma, including the appearance of "sarcomatous" tumor forms from originally solid carcinomas (for a comprehensive review see reference 39, and also for the in vitro and in vivo emergence

of different types of carcinomas from a given kind of bronchial tumor see references 14, 31). Such changes of the differentiation character of the cells in a given primary tumor are particularly problematic as their frequency seems to be often enhanced during therapy. If one makes the reasonable assumption that conversions of the differentiation type of one tumor cell type to another, as we describe for the NBT-II cell model in vitro, can also occur in vivo, it seems impossible to escape the corollary that the local environment of a tumor may not only influence its proliferation rate but also its state of differentiation and its metastatic potential.

We thank Dr. J. Gavrilovic for critical reading of the manuscript.

This work was supported by the Centre National de la Recherche Scientifique, the Association pour la Recherche contre le Cancer (ARC 6455), the Ligue Nationale Française contre le Cancer. A. M. Vallés is a fellow of the National Institutes of Health, Centre National de la Recherche Scientifique.

Received for publication 9 January 1989 and in revised form 7 June 1989.

References

1. Bader, B. L., L. Jahn, and W. W. Franke. 1988. Low level expression of cytokeratins 8, 18 and 19 in vascular smooth muscle cells of human umbilical cord and in cultured cells derived therefrom, with an analysis of the chromosomal locus containing the cytokeratin 19 gene. *Eur. J. Cell Biol.* 47:300–319.
2. Barrandon, Y., and H. Green. 1987. Cell migration is essential for sustained growth of keratinocyte colonies: the roles of transforming growth factor-α and epidermal growth factor. *Cell.* 50:1131–1137.
3. Behrens, J., W. Birchmeier, S. L. Goodman, and B. A. Imhof. 1985. Dissociation of Madin-Darby canine epithelial cells by the monoclonal antibody anti-Arc-1: mechanistic aspects and identification of the antigen as a component related to uvomorulin. *J. Cell Biol.* 101:1307–1315.
4. Ben-Ze'ev, A. 1984. Differential control of cytokeratins and vimentin synthesis by cell-cell contact and cell spreading in cultured epithelial cells. *J. Cell Biol.* 99:1424–1433.
5. Bologna, M., R. Allen, and R. Dulbecco. 1986. Organization of cytokeratin bundles by desmosomes in rat mammary cells. *J. Cell Biol.* 102:560–567.
6. Burridge, K. 1986. Substrate adhesion in normal and transformed fibroblasts: organization and regulation of cytoskeletal, membrane and extracellular matrix components at focal contacts. *Cancer Rev.* 4:18–78.
7. Chinkers, M., J. A. McKanna, and S. Cohen. 1979. Rapid induction of morphological changes in human carcinoma cells A431 by epidermal growth factor. *J. Cell Biol.* 83:260–265.
8. Chuong, C. -M., and G. M. Edelman. 1985. Expression of cell adhesion molecules in embryonic induction. II. Morphogenesis of adult feathers. *J. Cell Biol.* 101:1027–1043.
9. Cowin, P., W. W. Franke, C. Grund, H. -P. Kapprell, and J. Kartenbeck. 1985. The desmosome–intermediate filament complex. *In* The Cell in Contact. G. M. Edelman and J. P. Thiery, editors. John Wiley & Sons, New York. 427–460.
10. Cowin, P., H. -P. Kapprell, and W. W. Franke. 1985. The complement of desmosomal plaque proteins in different cell types. *J. Cell Biol.* 101:1442–1454.
11. Cowin, P., H. P. Kapprell, W. W. Franke, J. Tamkun, and R. O. Hynes. 1986. Plakoglobin: a protein common to different kinds of intercellular adhering junctions. *Cell.* 46:1063–1073.
12. Duband, J. L., T. Volberg, I. Sabanay, J. P. Thiery, and B. Geiger. 1988. Spatial and temporal distribution of adherens-junction associated adhesion molecule A-CAM during avian embryogenesis. *Development (Camb.).* 103:325–344.
13. Duden, R., and W. W. Franke. 1988. Organization of desmosomal plaque proteins in cells growing at low calcium concentrations. *J. Cell Biol.* 107:1049–1063.
14. Dunnill, M. S., and K. C. Gatter. 1986. Cellular heterogeneity in lung cancer. *Histopathology (Oxf.).* 10:461–475.
15. Edelman, G. M. 1984. Cell adhesion and morphogenesis: the regulatory hypothesis. *Proc. Natl. Acad. Sci. USA.* 81:1460–1464.
16. Edelman, G. M., B. A. Murray, R. M. Mege, B. A. Cunningham, and W. J. Gallin. 1987. Cellular expression of liver and neural cell adhesion molecules after transfection with their cDNAs results in specific cell-cell binding. *Proc. Natl. Acad. Sci. USA.* 84:8502–8506.
17. Feracci, H., and S. Maroux. 1980. Rabbit intestinal aminopeptidase N purification and molecular properties. *Biochim. Biophys. Acta.* 599: 448–463.
18. Fidler, I. J., and I. R. Hart. 1982. Biological diversity in metastatic neoplasms: origins and implications. *Science (Wash. DC).* 217:998–1003.
19. Franke, W. W., and R. Moll. 1987. Cytoskeletal components of lymphoid organs. I. Synthesis of cytokeratins 8 and 18 and desmin in subpopulations of extrafollicular reticulum cells of human lymph nodes, tonsils, and spleen. *Differentiation.* 36:145–163.
20. Franke, W. W., P. Cowin, M. Schmelz, and H. -P. Kapprell. 1986. The desmosomal plaque and the cytoskeleton. Junctional complexes of epithelial cells. *Ciba Found. Symp.* 125:26–48.
21. Franke, W. W., C. Grund, B. W. Jackson, and K. Illmensee. 1983. Formation of cytoskeletal elements during mouse embryogenesis. IV. Ultrastructure of primary mesenchymal cells and their cell-cell interactions. *Differentiation.* 25:121–141.
22. Franke, W. W., C. Grund, C. Kuhn, B. W. Jackson, and K. Illmensee. 1982. Formation of cytoskeletal elements during mouse embryogenesis. III. Primary mesenchymal cells and the first appearance of vimentin filaments. *Differentiation.* 23:43–59.
23. Franke, W. W., H. P. Kapprell, and P. Cowin. 1987. Plakoglobin is a component of the filamentous subplasmalemmal coat of lens cells. *Eur. J. Cell Biol.* 43:301–315.
24. Franke, W. W., D. Mayer, E. Schmid, H. Denk, and E. Borenfreund. 1981. Differences of expression of cytoskeletal proteins in cultured rat hepatocytes and hepatoma cells. *Exp. Cell Res.* 134:345–365.
25. Franke, W. W., E. Schmid, C. Grund, H. Müller, I. Engelbrecht, R. Moll, J. Stadler, and E. -D. Jarasch. 1981. Antibodies to high molecular weight polypeptides of desmosomes: specific localization of a class of junctional proteins in cells and tissues. *Differentiation.* 20:217–241.
26. Garcia, I., B. Sordat, E. Rauccio-Farinon, M. Dunand, J. P. Kraehenbuhl, and H. Diggelmann. 1986. Establishment of two rabbit mammary epithelial cell lines with distinct oncogenic potential and differentiated phenotype after microinjection of transforming genes. *Mol. Cell. Biol.* 6:1974–1982.
27. Garrod, D. R., E. P. Parrish, D. L. Mattey, J. E. Marston, H. R. Measures, and M. J. Vilela. 1989. Desmosomes: *In* The Cell in Contact. Morphoregulatory Molecules. G. M. Edelman, J. P. Thiery, and B. A. Cunningham, editors. John Wiley & Sons, New York. In press.
28. Geiger, B., K. T. Tokuyasu, A. H. Dutton, and S. J. Singer. 1980. Vinculin, an intracellular protein localized at specialized sites where microfilament bundles terminate at cell membranes. *Proc. Natl. Acad. Sci. USA.* 77:4127–4131.
29. Glenney, J. R., and P. Glenney. 1983. Fodrin is the general spectrin-like protein found in most cells whereas spectrin and the TW protein have a restricted distribution. *Cell.* 34:503–512.
30. Gorven, J. P., A. Rigal, J. Sarles, and S. Maroux. 1985. Aminopeptidase N and human blood group A antigenicity along the digestive tract and associated glands in the rabbit. *Cell Tissue Res.* 239:241–248.
31. Gould, V. E., V. A. Memoli, and L. E. Dardi. 1981. Multidirectional differentiation in human epithelial cancers. *J. Submicrosc. Cytol.* 13: 97–115.
32. Hennings, H., D. Michael, C. Cheng, P. Steinert, K. Holbrook, and S. H. Yuspa. 1980. Calcium regulation of growth and differentiation of mouse epidermal cells in culture. *Cell.* 19:245–254.
33. Heppner, G. H., and B. E. Miller. 1983. Tumor heterogeneity: biological implications and therapeutic consequences. *Cancer Metastasis Rev.* 2:5–23.
34. Kapprell, H. -P., K. Owaribe, and W. W. Franke. 1988. Identification of a basic protein of M_r 75,000 as an accessory desmosomal plaque protein in stratified and complex epithelia. *J. Cell Biol.* 106:1679–1691.
35. Kartenbeck, J., E. Schmid, W. W. Franke, and B. Geiger. 1982. Different modes of internalization of proteins associated with adhaerens junctions and desmosomes: experimental separation of lateral contacts induces endocytosis of desmosomal plaque material. *EMBO (Eur. Mol. Biol. Organ.) J.* 1:725–732.
36. Kartenbeck, J., K. Schwechheimer, R. Moll, and W. W. Franke. 1984. Attachment of vimentin filaments to desmosomal plaques in human meningiomal cells and arachnoidal tissue. *J. Cell Biol.* 98:1072–1081.
37. Kim, K. H., V. Stellmach, J. Javors, and E. Fuchs. 1987. Regulation of human mesothelial cell differentiation: opposing roles of retinoids and epidermal growth factor in the expression of intermediate filament proteins. *J. Cell Biol.* 105:3039–3051.
38. Kreis, T. E., and W. Birchmeier. 1980. Stress fibers sarcomeres of fibroblasts are contractile. *Cell.* 22:555–561.
39. Leith, J. T., and D. L. Dexter. 1986. Mammalian Tumor Cell Heterogeneity. CRC Press, Inc., Boca Raton, FL. 146 pp.
40. Lobach, D. F., T. Itoh, K. H. Singer, and B. F. Haynes. 1987. The thymic microenvironment. Characterization of in vitro differentiation of the IT26R21 rat thymic epithelial cell line. *Differentiation.* 34:50–59.
41. Mattey, D. L., and D. R. Garrod. 1986. Splitting and internalization of desmosomes in cultured kidney epithelial cells by reduction in calcium concentration. *J. Cell Sci.* 85:113–124.
42. Mattey, D. L., and D. R. Garrod. 1986. Calcium-induced desmosome formation in cultured kidney epithelial cells. *J. Cell Sci.* 85:95–111.
43. Moll, R., P. Cowin, H. -P. Kapprell, and W. W. Franke. 1986. Biology of disease. Desmosomal proteins: new markers for identification and classification of tumors. *Lab. Invest.* 54:4–25.
44. Nagafuchi, A., Y. Shirayoshi, K. Okazaki, K. Yasuda, and M. Takeichi.

1987. Transformation of cell adhesion properties by exogenously introduced E-cadherin cDNA. *Nature (Lond.)*. 329:341–343.
45. Neant, I., and P. Guerrier. 1988. Meiosis reinitiation of the mollusc Patella vulgata. Regulation of MPF, CSF, and chromosome condensation activity by intracellular pH, protein synthesis and phosphorylation. *Development (Camb.)*. 102:505–516.
46. Nelson, W. J., and P. J. Veshnock. 1986. Dynamics of membrane-skeleton (fodrin) organization during development of polarity in Madin–Darby canine kidney epithelial cells. *J. Cell Biol.* 103:1751–1766.
47. Nicolson, G. L. 1987. Tumor cell instability, diversification, and progression to the metastatic phenotype: from oncogene to oncofetal expression. *Cancer Res.* 47:1473–1487.
48. Ochs, B. A., W. W. Franke, R. Moll, C. Grund, M. Cremer, and T. Cremer. 1983. Epithelial character and morphologic diversity of cell cultures from human amniotic fluids examined by immunofluorescence microscopy and gel electrophoresis of cytoskeletal proteins. *Differentiation*. 24:153–173.
49. Overton, J. 1968. The fate of desmosomes in trypsinized tissue. *J. Exp. Zool.* 168:203–214.
50. Pasdar, M., and W. J. Nelson. 1988. Kinetics of desmosome assembly in Madin–Darby canine kidney epithelial cells: temporal and spatial regulation of desmoplakin organization and stabilization upon cell–cell contact. I. Biochemical analysis. *J. Cell Biol.* 106:677–685.
51. Penn, E. J., I. D. J. Burdett, C. Hobson, A. I. Magee, and D. A. Rees. 1987. Structure and assembly of desmosome junctions: biosynthesis and turnover of the major desmosome components of Madin–Darby canine kidney cells in low calcium medium. *J. Cell Biol.* 105:2327–2334.
52. Ramaekers, F. C. S., D. Haag, A. Kant, O. Moesker, P. H. K. Jap, and G. P. Vooijs. 1983. Coexpression of keratin- and vimentin-type intermediate filaments in human metastatic carcinoma cells. *Proc. Natl. Acad. Sci. USA*. 80:2618–2623.
53. Rheinwald, J. G., and T. M. O'Connell. 1985. Intermediate filament proteins as distinguishing markers of cell type and differentiated state in cultured human urinary tract epithelia. *Ann. NY Acad. Sci.* 455:259–267.
54. Rheinwald, J. G., T. M. O'Connell, N. D. Connell, S. M. Rybak, B. L. Allen-Hoffmann, P. J. La Rocca, Y. -J. Wu, and S. M. Rehwoldt. 1984. Expression of specific keratin subsets and vimentin in normal human epithelial cells. A function of cell type and conditions of growth during serial cuture. *Cancer Cells (Cold Spring Harbor)*. 1:217–228.
55. Rijsewijk, F., L. van Deemter, E. Wagenaar, A. Sonnenberg, and R. RAC mammary cell line results in morphological transformation and tumorigenicity *EMBO (Eur. Mol. Biol. Organ.) J.* 6:127–131.
56. Savino, W., M. Dardenne, M. Papiernik, and J. -F. Bach. 1982. Thymic hormone containing cells. Characterization and localization of serum thymic factor in young mouse thymus studied by monoclonal antibodies. *J. Exp. Med.* 156:628–633.
57. Schmelz, M., R. Duden, P. Cowin, and W. W. Franke. 1986. A constitutive transmembrane glycoprotein of M_r 165,000 (desmoglein) in epidermal and non-epidermal desmosomes. I. Biochemical identification of the peptide. *Eur. J. Cell Biol.* 42:177–183.
58. Schmid, E., W. W. Franke, C. Grund, D. L. Schiller, H. Kolb, and N. Paweletz. 1983. An epithelial cell line with elongated myoid morphology derived from bovine mammary gland. *Exp. Cell Res.* 146:309–328.
59. Schmid, E., D. L. Schiller, C. Grund, J. Stadler, and W. W. Franke. 1983. Tissue type-specific expression of intermediate filament proteins in a cultured epithelial cell line from bovine mammary gland. *J. Cell Biol.* 96:37–50.
60. Stoker, M., and M. Perryman. 1985. An epithelial scatter factor released Nusse. 1987. Transfection of the int-1 mammary oncogene in cuboidal by embryo fibroblasts. *J. Cell Sci.* 77:209–223.
61. Stoker, M., E. Gherardi, M. Perryman, and J. Gray. 1987. Scatter factor is a fibroblast-derived modulator of epithelial cell mobility. *Nature (Lond.)*. 327:239–242.
62. Strauli, P., and L. Weiss. 1977. Perspectives in cancer research. Cell locomotion and tumor penetration. *Eur. J. Cancer*. 13:1–12.
63. Sun, T. -T., P. Bonitz, and W. H. Burns. 1984. Cell culture of mammalian thymic epithelial cells: growth, structural and antigenic properties. *Cell. Immunol.* 83:1–13.
64. Takeichi, M. 1987. Cadherins: a molecular family essential for selective cell–cell adhesion and animal morphogenesis. *Trends Genet.* 3:213–217.
65. Takeuchi, S. 1987. Cytochalasin B affects selectively the marginal cells of the epithelial sheet in culture. *Zool. Sci. (Tokyo)*. 4:465–474.
66. Tchao, R. 1982. Novel forms of epithelial cell motility on collagen and on glass surfaces. *Cell Motil.* 4:333–341.
67. Thiery, J. P. 1984. Mechanisms of cell migration in the vertebrate embryo. *Cell Differ.* 15:1–15.
68. Thiery, J. P., G. C. Tucker, and H. Aoyama. 1985. Gangliogenesis in the avian embryo: migration and adhesion properties of neural crest cells. *In* Molecular Basis of Neural Development. G. M. Edelman, W. M. Gall, and W. M. Cowan, editors. John Wiley and Sons, New York. 181–211.